

A&A manuscript no.
(will be inserted by hand later)

Your thesaurus codes are:
07 (08.16.4; 08.15.1; 08.09.2 HS 2324+3944)

ASTRONOMY
AND
ASTROPHYSICS

The photometric behaviour of the peculiar PG 1159 star HS 2324+3944 at high frequency resolution [★]

R. Silvotti¹, S. Dreizler², G. Handler³, and X.J. Jiang⁴

¹ Osservatorio Astronomico di Capodimonte, via Moiariello 16, I-80131 Napoli, Italy

² Institut für Astronomie und Astrophysik, Waldhäuser Straße 64, D-72076 Tübingen, Germany

³ Institut für Astronomie, Universität Wien, Türkenschanzstraße 17, A-1180 Wien, Austria

⁴ Beijing Astronomical Observatory and United Laboratory of Optical Astronomy, CAS, Beijing 100012, China

Received; accepted

Abstract. We present the results from 135 hours of nearly continuous time series photometry on the “hybrid” (H-rich) PG 1159 variable star HS 2324+3944, obtained in August–September 1997. The power spectrum of the data shows several frequencies (about 20 or more), concentrated in three narrow and very crowded regions near 475, 390 and 950 μHz in decreasing amplitude order. Most (if not all) of the peaks in the latter region are linear combinations of the high-amplitude frequencies between 455 and 500 μHz . If we divide the data set into two equal parts, the power spectra are different. This is probably due to a not sufficiently long (and therefore not completely resolved) light curve; nevertheless an alternative hypothesis of a single damped oscillator may not be completely ruled out. If we adopt the first hypothesis, the high concentration of peaks between 455 and 500 μHz suggests the presence of both $l=1$ and $l=2$ high-overtone nonradial g-modes. The insufficient frequency resolution of our data does not allow to obtain definite precision asteroseismology results. Nevertheless a spacing of the signals is observed, probably due to stellar rotation with a period of 2.3 days. If the signal spacing was due to the successive overtones, the period spacings would be equal to 18.8 ($l=1$) and 10.4 ($l=2$) s.

Key words: stars: post-AGB - stars: oscillations - stars: individual: HS 2324+3944

1. Introduction

1.1. Pulsating and nonpulsating PG 1159 stars

The stars of the PG 1159 spectral class (31 members) constitute the intermediate evolutionary phase between the

end of the constant luminosity phase – at the tip of the asymptotic giant branch (AGB) – and the beginning of the white dwarf (WD) cooling phase. Probing their interior structure provides direct constraints on both classes of stars and may help to understand better the transition from AGB to WDs and the nuclear burning turn off process. A powerful method to probe the interior structure of the pre-WD stars and to determine some of their basic stellar parameters is given by asteroseismology. This is possible because 15 PG 1159 stars and central stars of planetary nebulae (CSPN) of type [WC], called GW Vir stars from the prototype (PG 1159-035), show multiperiodic luminosity variations which have been interpreted as nonradial g-mode pulsations. Among them, ten are CSPN, while five appear not to be surrounded by a nebula (Bradley 1998). The nature of the luminosity variations of the GW Vir stars was first proven to be stellar pulsation in the case of PG 1159-035 itself (Winget et al. 1991). Nevertheless, and despite the successful results from adiabatic models to which we will refer to below, the pulsation mechanism of the GW Vir stars is still not well understood. Although almost all authors agree that the pulsations should be driven by the κ - γ mechanism, based on the C/O cyclic ionization (Starrfield et al. 1984), a good agreement between spectroscopic abundances and observed pulsation periods has not been yet found (Bradley & Dziembowski 1996). A new element in this picture was recently added by Dreizler & Heber (1998): their results suggest that the GW Vir pulsations could be related to the nitrogen abundance. On the other hand, in the adiabatic pulsation field, theory may explain several observed phenomena as frequency splitting due to rotation and/or magnetic fields, period spacing of successive overtones, and variations around the average period spacing caused by mode trapping in the outer layers of the star (Kawaler & Bradley 1994 and references therein). However, the measurement of frequency and period spacing, which leads to accurate determination of rotation, weak magnetic fields, stellar mass, external layer masses, and even luminosity and distance, needs power spectra with low noise and high frequency resolu-

Send offprint requests to: R. Silvotti (silvotti@na.astro.it)

[★] Based on observations obtained at the McDonald, Loiano and Beijing Observatories and at the German-Spanish Astronomical Center, Calar Alto, operated by the Max-Planck-Institut für Astronomie Heidelberg jointly with the Spanish National Commission for Astronomy.

arXiv:astro-ph/9811178v1 11 Nov 1998

tion. For these reasons it is necessary to obtain long and nearly continuous data sets, such as those obtained by the Whole Earth Telescope network (Nather et al. 1990).

1.2. *HS 2324+3944*

The star HS 2324+3944 (hereafter HS 2324) is one out of four peculiar members of the PG 1159 spectral class showing strong H Balmer absorption in their spectra (Dreizler et al. 1996), called “hybrid PG 1159 stars” (Napiwotzki & Schönberner 1991) or IgEHPG 1159, following the notation scheme of Werner (1992). It has an effective temperature of $(130\,000 \pm 10\,000)$ K and a surface gravity $\log g = 6.2 \pm 0.2$ (Dreizler et al. 1996). Recent new analysis of the HST-GHRS spectrum of HS 2324 show that the C/He and O/He ratio (0.4 and 0.04 by number) is as high as in ordinary PG 1159 stars (Dreizler 1998). Therefore only the hydrogen abundance (H/He=2 by number) makes it unusual. HS 2324 does not show direct signs of ongoing mass loss from P Cygni shaped line profiles, like several other luminous PG 1159 stars (Koesterke et al. 1998). However, detailed line profiles from high resolution Keck spectroscopy show evidence of mass loss in the order of roughly $10^{-8} M_{\odot}/yr$ (Dreizler et al., in preparation). Regarding effective temperature and gravity, it belongs to the subgroup of luminous PG 1159 stars which are in general Central Stars of Planetary Nebulae. However, differently from all the other known hybrid PG 1159 stars, no nebula is detected around HS 2324 (Werner et al. 1997).

HS 2324 was discovered to be variable by Silvotti (1996). Handler et al. (1997), with more extensive observations, showed that at least four different frequencies were active and therefore that the GW Vir hypothesis was the most likely. For other two hybrid PG 1159 stars, the nuclei of A 43 and NGC 7094, periodic light variations are only suspected (Ciardullo & Bond 1996). The interest for the variability of HS 2324 is enhanced by its hydrogen abundance. The presence of H was generally considered as a inhibitor of pulsations (Stanghellini et al. 1991). First steps to test the effects of the presence of H in the driving regions have been undertaken by Saio (1996) and Gautschy (1997). The models of Saio (1996) do pulsate with 3% of H mass fraction. The models of Gautschy (1997) are able to reproduce the observed periods of HS 2324, with a very similar H abundance of 20% by mass.

For all the reasons stated above, HS 2324 is a very interesting star: the analysis of its photometric behaviour at high frequency resolution may give important results not only for a detailed study of the star itself, but also for more general questions regarding the GW Vir pulsation phenomenon. Therefore we decided to carry out a multisite photometric campaign on HS 2324, which may be considered as a first step for successive more extensive campaigns.

2. Observations

The multisite campaign on HS 2324 was performed during 2 weeks in August–September 1997, centered on new Moon. The journal of observations in Table 1 gives information on the observatories involved, telescopes and instruments used, and duration of the single runs. Most observations were obtained using two or three channel photometers with bialkali photomultipliers (EMI9784QB for Loiano, Hamamatsu R647 for Beijing and McDonald), no filters, and an integration time of 10 s, which was subsequently merged to 90 s. The leak of sensitivity to periods shorter than 180 s did not give us any trouble because no signals were detected in that range from a preliminary analysis of the photometer data alone. Only the Calar Alto data were collected using a SITE#1d CCD, B filter, and an exposure time of about 20 s (first two nights) or 40 s (following three nights) for each datum; the times between successive data points vary between about 70 and 100 s. The error introduced by the different effective wavelengths of each detector has been evaluated to be not more than 5% in amplitude.

Despite the small number of participants in the campaign, only four, we obtained a good coverage, comparable with other multisite campaigns, thanks to the good weather conditions in most nights at the different sites. The complete (and combined) light curve is shown in Figure 1; it has a total duration of 134.9 hours, with an overall duty cycle of 43%. In the central part of the run (40.8 hours), the duty cycle is 98%.

2.1. *Details on data acquisition and reduction*

We followed basically the same data reduction procedure as described in Handler et al. (1997). Here we summarize this procedure and give some detail on a few differences.

For the Beijing and McDonald photoelectric data, we chose the same comparison star already used by Handler et al. (1997), which was also one of the comparison stars used in the Calar Alto CCD measurements. For the Loiano photoelectric data this was not possible because the box of channel 2 is more distant from channel 1: therefore we used the same comparison star already used by Silvotti (1996). Both comparison stars were tested again for photometric constancy and found not to be variable. We then turned to sky subtraction. For the Beijing measurements, where a third channel was available, the sky background could be monitored simultaneously. In this case we subtracted the sky counts on a point by point basis. To reduce the scatter of the background measurements, some smoothing was applied whenever possible. At McDonald and Loiano only two channels were available. In this case sky was measured using channel 1 and 2 for about 1 min at irregular intervals of typically 20–90 min, depending on sky stability and presence of the Moon. The sky counts were then interpolated linearly and subtracted. In a few cases we

Table 1. Journal of the observations

Telescope	Instrument	Observer	Date (UT)	Start Time (UT)	Run Length (hours)
McDonald 2.1 m	PMT	GH	26 Aug 1997	07:31:20	3.55
McDonald 2.1 m	PMT	GH	27 Aug 1997	04:45:00	6.33
Loiano 1.5 m	PMT	RS	27 Aug 1997	20:19:16	3.54
McDonald 2.1 m	PMT	GH	28 Aug 1997	03:16:00	7.66
McDonald 2.1 m	PMT	GH	29 Aug 1997	03:10:30	7.59
Loiano 1.5 m	PMT	RS	29 Aug 1997	23:32:57	1.00
Loiano 1.5 m	PMT	RS	30 Aug 1997	21:57:57	4.84
McDonald 0.9 m	PMT	GH	31 Aug 1997	03:49:30	0.58
Loiano 1.5 m	PMT	RS	31 Aug 1997	22:01:01	5.00
Beijing 0.85 m	PMT	JX	01 Sep 1997	16:17:20	1.03
Calar Alto 2.2 m	CCD	SD	01 Sep 1997	19:58:51	8.98
Loiano 1.5 m	PMT	RS	01 Sep 1997	21:30:01	5.49
Beijing 0.85 m	PMT	JX	02 Sep 1997	11:59:40	8.39
Loiano 1.5 m	PMT	RS	02 Sep 1997	20:05:19	4.29
Calar Alto 2.2 m	CCD	SD	02 Sep 1997	22:16:23	6.20
McDonald 0.9 m	PMT	GH	03 Sep 1997	02:39:40	8.73
Beijing 0.85 m	PMT	JX	03 Sep 1997	12:04:20	8.27
Calar Alto 2.2 m	CCD	SD	03 Sep 1997	20:30:41	8.29
Beijing 0.85 m	PMT	JX	04 Sep 1997	16:03:30	4.10
Loiano 1.5 m	PMT	RS	04 Sep 1997	19:23:35	5.77
Calar Alto 2.2 m	CCD	SD	04 Sep 1997	19:32:06	9.28
McDonald 0.9 m	PMT	GH	05 Sep 1997	05:31:30	1.76
Calar Alto 2.2 m	CCD	SD	05 Sep 1997	19:32:18	8.82
McDonald 0.9 m	PMT	GH	06 Sep 1997	02:39:10	8.77
McDonald 0.9 m	PMT	GH	07 Sep 1997	06:05:00	5.38
McDonald 0.9 m	PMT	GH	08 Sep 1997	02:25:40	9.10

used a cubic spline for the sky interpolation, when it was clear that this procedure was giving better results than the linear fit. All the PMT data were then corrected for extinction. Afterwards, they were used to examine possible transparency variations. In a few cases of high sky instability, the count ratio between channel 1 and channel 2 was used instead of channel 1 counts only. Some smoothing of the channel 2 data was applied when possible. Systematic long time scale trends (> 2 hours), probably due to tube drifts and/or to residual extinction, were finally compensated by means of linear or cubic spline interpolation.

For the Calar Alto CCD data, 10 comparison stars were selected, after having been tested for photometric constancy. Their average magnitude was subtracted from the HS 2324 measurements on a point by point basis. Differential extinction was corrected by means of a cubic spline.

Finally all the single data sets (PMT + CCD) were set to a mean value of zero. The times of all data were then converted to Barycentric Julian Date using the algorithm of Stumpff (1980). The accuracy of the original times was of the order of ± 0.3 s (Beijing), ± 0.01 s (Loiano), ± 0.2 s (McDonald) and ± 1 s (Calar Alto). For Calar Alto 1 s is also the time accuracy of each measurement. Moreover, to have a more homogeneous data set, we have binned

the PMT data to an effective integration time of 90 s. The value of 90 s has been chosen because it corresponds to the mean distance between consecutive CCD observations. When more than one site was active at the same time, in the overlap regions, we applied a weighted average of the data obtained at the different sites. In this way even lower quality data can be used to improve the S/N ratio (see Moskalik 1993). In its final form, the data set is constituted by the time of each integration, the fractional departure of the count rate from the mean (modulation intensity), and the error.

3. Temporal spectroscopy

3.1. Spectral window and power spectrum

We computed a single sine function with unit amplitude at the same sample times of the entire data set (window function). The discrete Fourier transform of the window function gives the spectral window, which is shown in Figure 2. For more completeness, both the amplitude and the power (amplitude squared) spectra of the window function are presented. The only structures which may give troubles for the unambiguous identification of the modes are the 1 cycle/day aliases, with a relative amplitude of about 0.3 (relative power of 0.09).

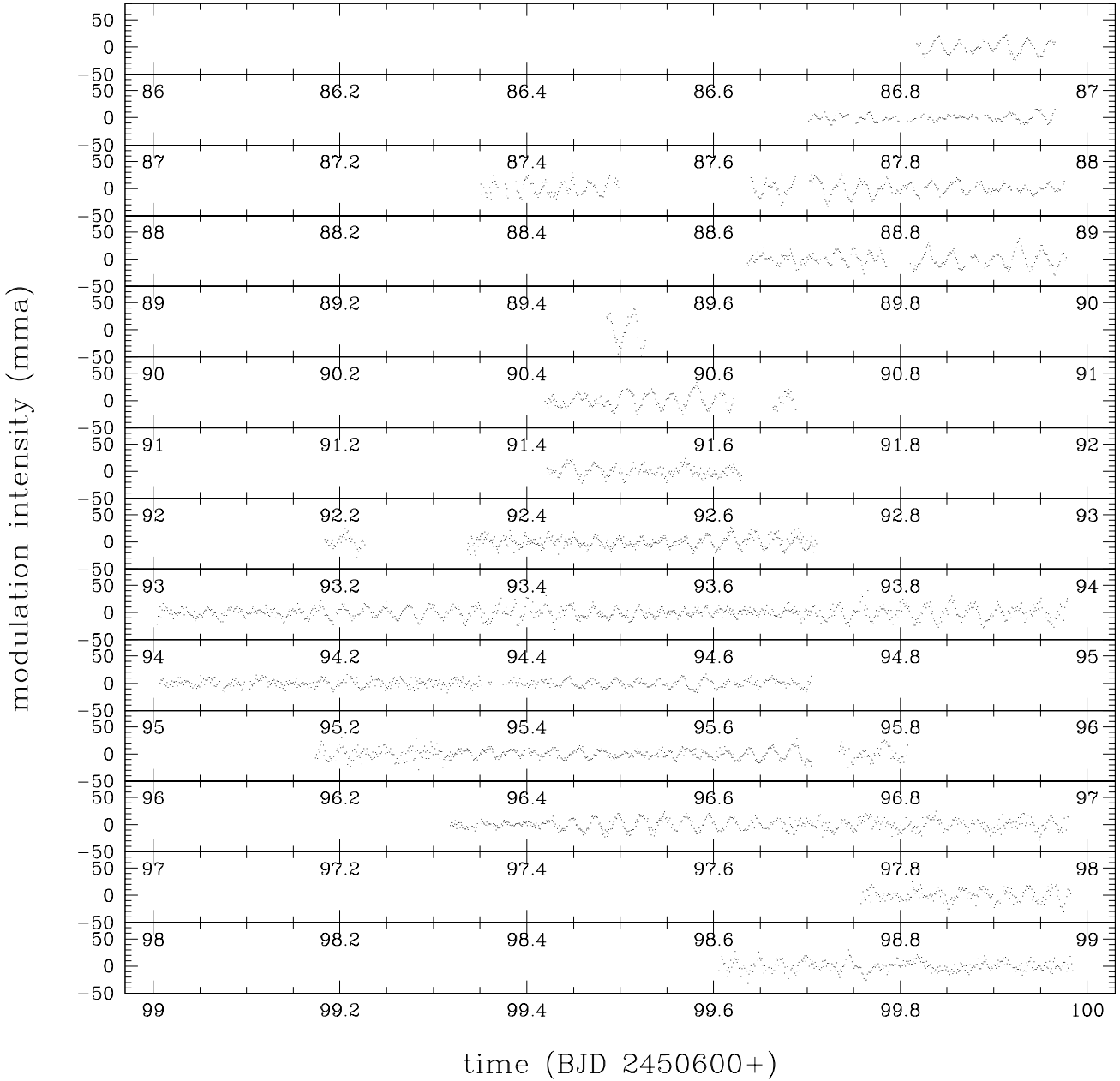


Fig. 1. The complete light curve of HS 2324; each panel represents 24 hours.

Using the same discrete Fourier transform (DFT), based on the Deeming (1975) method and Kurtz (1985) algorithm, we computed the transform of the entire reduced data set. In Figure 2 both amplitude and power spectrum are shown in units of millimodulation amplitude (mma) and micromodulation power (μmp), following the suggestion of Winget et al. (1994). We clearly see that the signals are concentrated in three main regions near 390, 470 and 950 μHz . These regions are highlighted in Figure 3. The tested frequency resolution of our data set is 1.4 μHz , according to Loumos & Deeming (1978); such a

value corresponds to obtain a half amplitude separation of two close peaks with equal amplitude.

Looking at Figure 3, some structures appear to be not completely resolved, suggesting that the light curve could be too short that we can resolve all the present frequencies. To test this crucial point, we divided the data set into two equal parts and computed the Fourier transform of each part. The two power spectra, presented in Figure 4, show strong differences not only in amplitude, but also in frequency. The first interpretation of such differences is simply that the data set is not long enough to “stabilize”

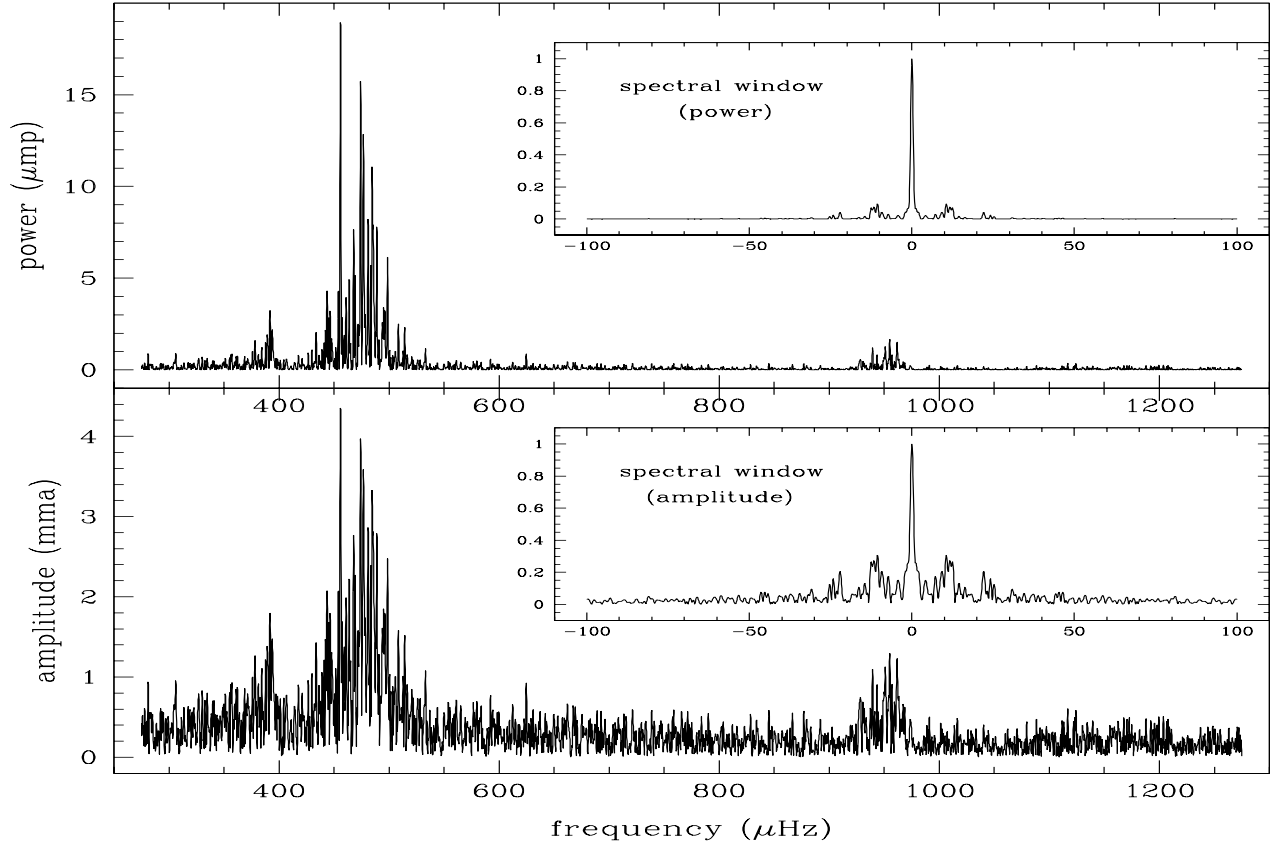


Fig. 2. Power spectrum (top) and amplitude spectrum (bottom) of the entire data set. The DFT of the window function (spectral window) is also reported both in power and in amplitude; we can note that the 1 cycle/day sidelobes have maxima at $\pm 10.6 \mu\text{Hz}$, corresponding to a period of 1.09 days.

the Fourier transform. In other words, the light curve is not completely resolved. The reliability of this hypothesis is increased by the fact that our best multisinusoidal fit of the entire data set (see next section and Table 2) gives good results also when applied only to the first or the second half of data (Figure 4). If the DFT apparent instability is actually due to the insufficient coverage, most of the analyses reported in sections 3.2, 4.1 and 4.2, and based on the assumption that the DFT of HS 2324 is not time dependent on time scales shorter than our run, will need further confirmation from a new longer observational campaign.

On the other hand, if the DFT time instability was real, we would need a different explanation for such peculiar behaviour. An alternative hypothesis of a fast damped oscillator has been considered and is reported in Section 5.

3.2. Frequency identification

Looking at Figure 2 and 3, it is immediately evident that determining the active frequencies from the power spectrum of HS 2324 will be more difficult than in most other

GW Vir stars for several reasons: the power is concentrated in only 3 crowded regions; the amplitudes are very low; the low frequencies imply that the frequency and the period spacing expected may have about same values. The high frequency region does not help much because it seems to be constituted only by linear combinations of the low-frequency peaks. Moreover we know that the frequencies are not completely resolved and therefore we certainly have errors both in frequency and in amplitude.

To distinguish the real frequencies present in the HS 2324 data from the artifacts introduced by the spectral window, we proceeded as follows. First we selected the highest peak in each of the three “active regions” near 390, 470 and 950 μHz . The separation of the three active regions guarantees that the aliases of each frequency have almost zero influence in the other two regions. Second we applied a least-squares multisinusoidal fit to the data to determine accurate amplitudes and phases of the three selected sine waves. Third we created an artificial signal adding together the three sinusoids and using the same sampling times as the data. This artificial signal was then subtracted from the data (prewhitening), and the residuals were analyzed again. Three (or less) new frequencies

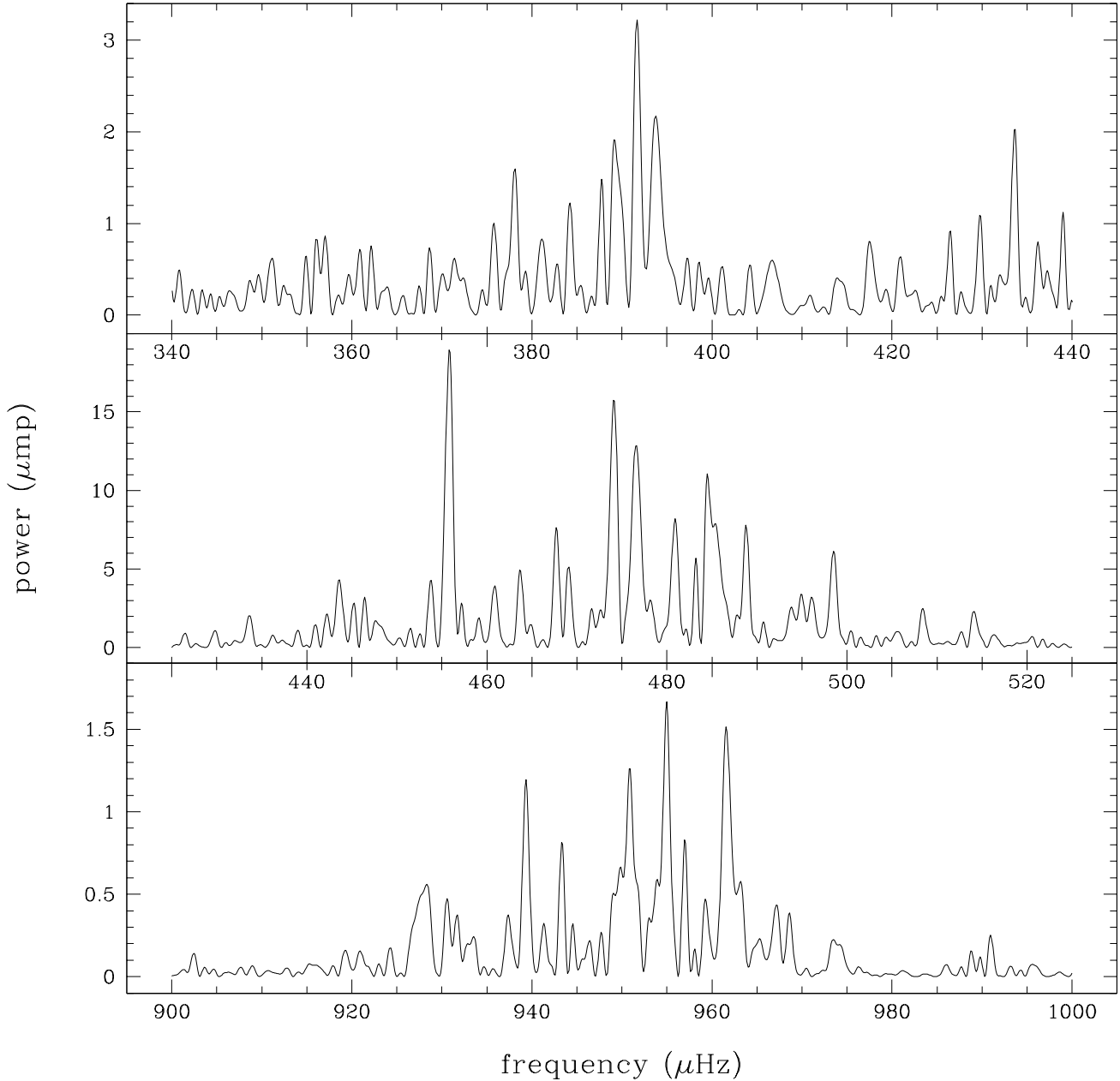


Fig. 3. Detailed power spectrum of the entire data set. Note that different vertical scales have been used.

were selected and the whole procedure was repeated n times until the power of the prewhitened data was near the level of the noise. At each iteration we selected first those frequencies which were not coincident with the one day aliases of the strongest signals. At the end of the whole process, the frequencies, amplitudes and phases were optimized with a final least-squares fit with all the frequencies found. The resulting best fit parameters are listed in Table 2. It is important to emphasize, however, that the solution in Table 2 is not the only one. After having performed the prewhitening of 7 frequencies (marked with an

asterisk in Table 2), different solutions become possible. The frequencies selected in Table 2 represent the result of several attempts. The solution that we have chosen has the advantage that it produces small residuals with a relative small number of frequencies (Figure 5). Looking at Table 2, we can note that most (if not all) of the high frequency signals correspond to linear combinations of the high-amplitude frequencies.

4. “Classical” seismological interpretation

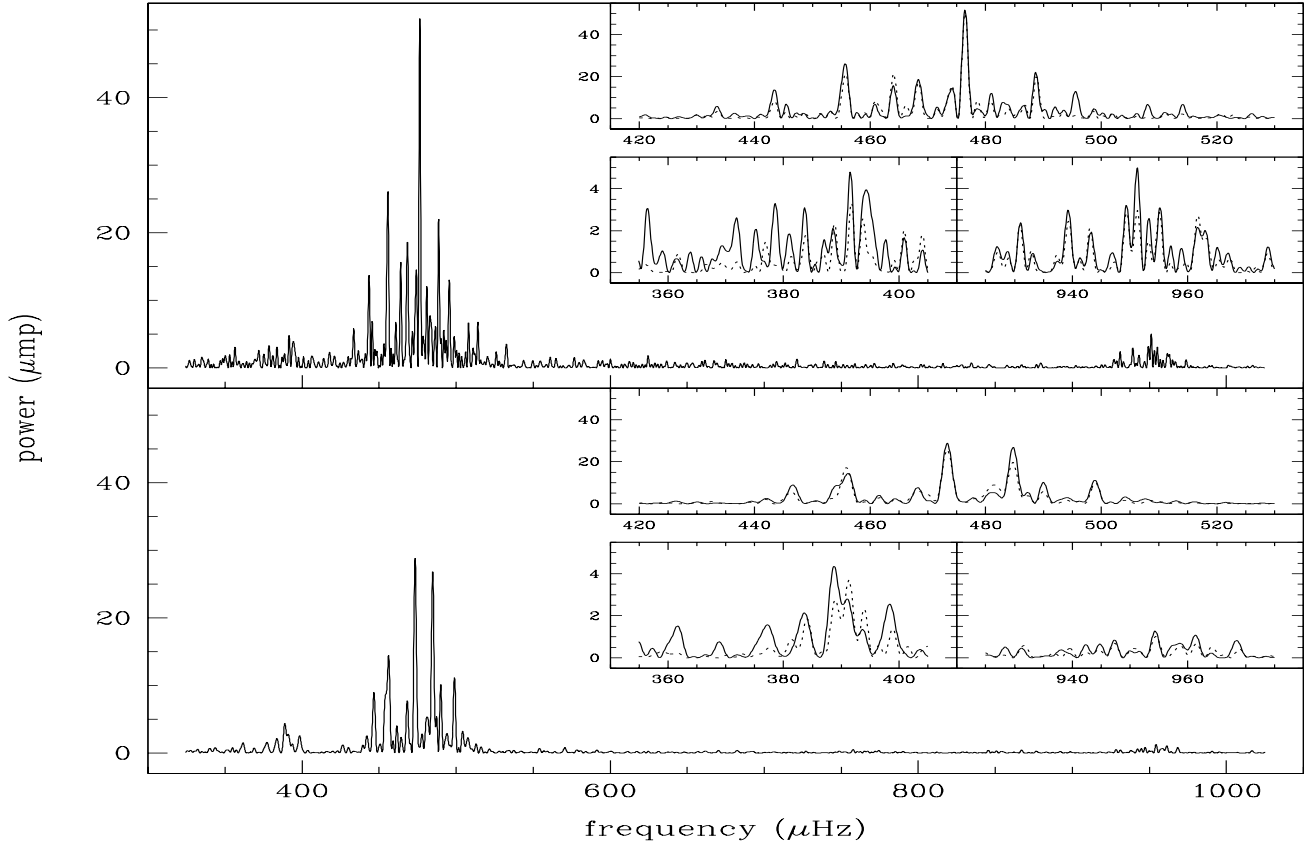


Fig. 4. Power spectrum of the first half of data (top) versus second half (bottom). Note the strong differences both in power and in frequency. In the small panels the regions of interest are highlighted; the dotted lines represent the spectra of the first and second half of a synthetic light curve obtained summing the 19 sinusoids listed in Table 2 and having same time sampling as the HS 2324 data. No noise was added to the synthetic light curves.

4.1. Frequency splitting

In the power spectrum of HS 2324 there is not any clear direct sign of frequency splitting. This may be due to different reasons. A very small rotation rate, with secondary ($m \neq 0$) modes below the frequency resolution, seems quite unlikely because it would require a rotation period longer than about 9 days. A more realistic possibility is that the star has a low inclination, so that the amplitudes of the $m \neq 0$ modes are near the level of the noise. A third possibility is that the concentration of the peaks is so high that we are simply not able to recognize the modes splitted by the rotation.

If a direct identification of the rotational splitting is not possible, the high number of peaks allows one to make use of statistical methods. First we constructed an histogram of the frequency separations between the signals listed in Table 2, excluding the linear combinations. The result was not significant: no preferred frequency spacings appeared. Another attempt was done using all the peaks of the power spectrum higher than a fixed level; we selected 49 frequencies and made the histogram. Here also we did

not get any significant result apart that all the peaks were never higher than the one day alias near 10–11 μHz .

At this point we invoked a third method: we computed the DFT of the amplitude spectrum, using two different subsets spanning 350–1000 μHz (all signals) and 440–500 μHz (only high power signals). The resulting power spectra are shown in Figure 6 (left panels). Considering the lower panel, the highest peaks are at 10.1 and 4.2 μHz ; a third peak at 2.5 μHz is clearly visible and more evident in the upper panel. Let us focus our attention to the latter two (for the first one we will give an interpretation below): their ratio, equal to 0.594 (or 0.589), is very close (1% level) to the canonical value of 0.6 predicted by asymptotic theory for the ratio between $l=1$ and $l=2$ rotational frequency splitting. Therefore the 4.2 and 2.5 μHz peaks might correspond to the frequency separation between m and $m \pm 1$ ($l=2$ and $l=1$) modes. The corresponding rotation period of the star would be $P_{ROT} = 2.31 \pm 0.15$ days. This result may not be considered definitive because the method used is very sensitive to noise. Moreover the signal that we are looking for is not actually coherent: the constant frequency separation between the modes of the same

Table 2. Results of the sinusoidal fit

Frequency (μHz)	Period (s)	Amplitude (mma)	T_{MAX}^1 (BJD 2450686.+)	Comments
389.27 \pm 0.06	2568.89 \pm 0.41	1.33 \pm 0.15	0.82337 \pm 0.00145	f1
* 391.64 \pm 0.06	2553.38 \pm 0.37	1.50 \pm 0.15	0.84665 \pm 0.00135	f2
393.51 \pm 0.06	2541.25 \pm 0.37	1.45 \pm 0.15	0.82707 \pm 0.00133	f3
* 455.74 \pm 0.02	2194.23 \pm 0.10	4.27 \pm 0.15	0.83075 \pm 0.00041	f4
460.68 \pm 0.06	2170.70 \pm 0.27	1.84 \pm 0.16	0.83464 \pm 0.00117	f5
472.90 \pm 0.05	2114.63 \pm 0.23	3.28 \pm 0.23	0.82214 \pm 0.00098	f6
* 473.87 \pm 0.05	2110.29 \pm 0.24	3.29 \pm 0.22	0.82515 \pm 0.00097	f7
476.13 \pm 0.04	2100.25 \pm 0.19	4.69 \pm 0.45	0.84137 \pm 0.00089	f8
* 476.64 \pm 0.04	2098.02 \pm 0.17	5.20 \pm 0.45	0.84039 \pm 0.00078	f9
480.95 \pm 0.04	2079.22 \pm 0.18	2.25 \pm 0.15	0.83641 \pm 0.00077	f10
485.11 \pm 0.03	2061.37 \pm 0.14	3.13 \pm 0.17	0.83581 \pm 0.00061	f11
498.78 \pm 0.04	2004.91 \pm 0.18	1.98 \pm 0.15	0.82382 \pm 0.00082	f12
930.49 \pm 0.11	1074.71 \pm 0.13	1.02 \pm 0.21	0.82086 \pm 0.00109	(f4+f7)
931.71 \pm 0.12	1073.29 \pm 0.13	0.94 \pm 0.20	0.82618 \pm 0.00111	f4+f8 (f4+f9)
* 939.42 \pm 0.11	1064.49 \pm 0.13	1.08 \pm 0.21	0.81967 \pm 0.00105	(f4+f11)
949.25 \pm 0.16	1053.46 \pm 0.17	0.76 \pm 0.22	0.82672 \pm 0.00144	f6+f8 (f6+f9)
* 955.04 \pm 0.10	1047.07 \pm 0.11	1.22 \pm 0.20	0.82392 \pm 0.00091	f7+f10 (f4+f12)
* 961.71 \pm 0.12	1039.82 \pm 0.13	1.04 \pm 0.22	0.81880 \pm 0.00120	f9+f11 (f10+f10)
963.15 \pm 0.13	1038.26 \pm 0.14	0.96 \pm 0.21	0.82792 \pm 0.00120	

Notes: ⁽¹⁾ Time of the first maximum inside the data set. ^(*) These frequencies are the most reliable (see the text).

overtone splitted by the rotation does not correspond, in general, to the separation between successive overtones, which is not constant in frequency (but almost constant in our particular case, due to the narrowness of the high-power region). From this point of view a more appropriate – but not much less noisy – method to measure the frequency spacing is given by the autocorrelation of the DFT (Press et al. 1992). The results of the DFT autocorrelation, reported in Figure 6 (right panel), are less significant than, but do not contradict, those obtained from the DFT of the amplitude spectrum.

Looking now at the peak near 10 μHz of Figure 6, its frequency separation is very close to that of the one day alias; therefore we could conclude that it is actually produced by all the aliases of the signals. This conclusion would give more confidence in the rotational origin of the two peaks at 4.2 and 2.5 μHz . Moreover comparing the power of these two peaks with that of the one day alias, we could suppose that the weakness of the $m \neq 0$ modes is actually due to the low inclination of the star. But with a deeper analysis (testing the variations of the three peaks of Figure 6 (left panels) when we subtract different signals from the HS 2324 data (prewhitening)), we can easily demonstrate that the peak at about 10 μHz has at least two components: one at 10.6 μHz actually related to the one day alias and another one related to the separation between the two signals at about 474 and 485 μHz in the data DFT. Therefore it is more difficult to derive any consideration about the weakness of the $m \neq 0$ modes and the low inclination hypothesis does not have any support. On the other hand, we can also demonstrate that the origin of

the 2.5 and 4.2 μHz peaks is strongly related to the separation between a few large amplitude signals. Conclusion: if the frequency spacings of 2.5 and 4.2 μHz are actually due to the stellar rotation, the low inclination hypothesis can not be longer followed. The new even more simple picture would be the following: there are five $l=1$ triplet component candidates (474.1 ¹ and 476.6 μHz plus 389.1, 391.7 and 393.8 μHz) and there are three $l=2$ quintuplet component candidates (480.9, 484.5 and 488.8 μHz). If we derive the frequency spacing from these values we obtain a rotation period of the star $P_{ROT} = 2.41 \pm 0.22$ days, slightly different from the previous one. Other possible multiplets might be present at 483.2 and 485.4 μHz ($l=1$), and 463.7 and 467.7 μHz ($l=2$).

In this context we can also try to estimate the inclination of the star using the $l=1$ modes. Following Pesnell (1985) ² we obtain an indication for $i \simeq 50^\circ$.

4.2. Period spacing and mode trapping

The two peaks in the amplitude spectrum DFT, described in the previous section, could also be due to the period

¹ The frequencies reported here are not taken from Table 2; we prefer to use the values found in the data DFT, as Table 2 may contain errors.

² These equations require two strong assumptions, certainly not completely – if not at all – realistic for low gravity GW Vir stars: the $m \neq 0$ modes should be all excited at the same amplitude level; the amplitude variations during the run must be excluded. Therefore this estimate of the inclination of the stellar rotational axis must be considered very tentative.

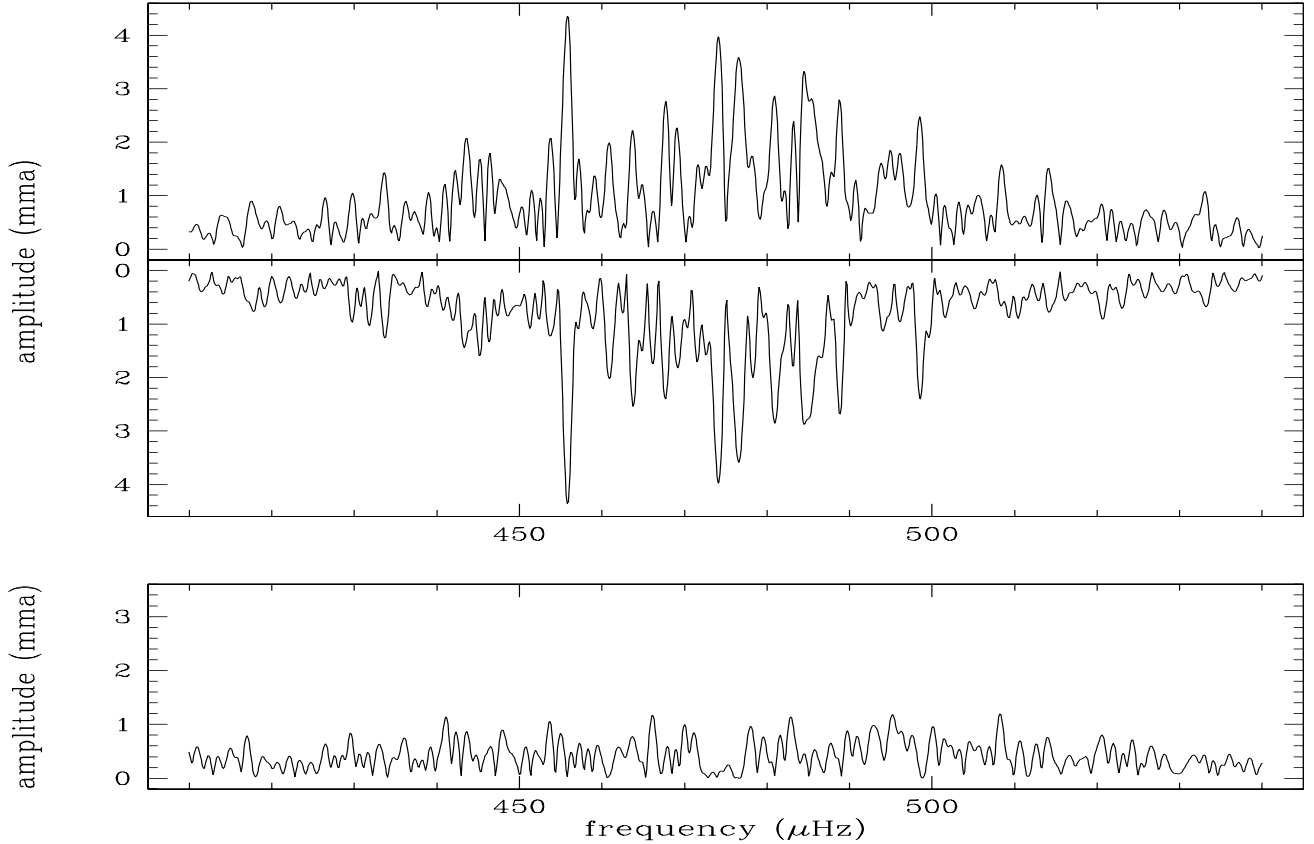


Fig. 5. Upper panels: amplitude spectrum of the entire data set (top) compared with the spectrum of the 19-frequency fit (bottom) having the same time sampling as the data. No noise was added to the synthetic data. Lower panel: spectrum of the residuals. Note that the vertical scale is the same in all panels.

spacing between modes with successive overtones. In Figure 7 (left panels) we show the DFT of the period spectrum (amplitude spectrum in the period domain). For the upper panel we used a subset of the period spectrum with periods between 1000 and 2857 s, while for the lower panel we used a narrower part with periods spanning 2000–2273 s. Excluding the peak at about 46 s, which is related to the one day alias as discussed in the previous section, the most significant period spacings are 18.8 s and 10.4 s (at least in the lower graph; in the upper graph the 10.4 s peak appears more uncertain). Their ratio is close (accuracy better than 5%) to the asymptotic value of $\sqrt{3}$, suggesting that 18.8 and 10.4 s might correspond to the $l=1$ and $l=2$ period spacings. In this hypothesis, the differences between the two left panels of Figure 7 suggest that the $l=2$ modes might be present only (or mainly) in the high-amplitude region between 2000 and 2273 s.

An attempt to confirm the hypothesis that the modes of HS 2324 are equally spaced in period (and not in frequency) has been done applying the Kolmogorov-Smirnov (K-S) test (Kawaler 1988) and the Inverse Variance technique (O’Donoghue 1994) to the first 12 periods listed in Table 2 (excluding the linear combinations). The results,

reported in Figure 7 (right panels), do not confirm that the modes are equally spaced in period. Moreover, the lack of any significant period spacing further indicates that the period list is not complete³.

Nothing may be said about the trapped modes phenomenon apart the following. The ratio between the frequencies of the highest peaks in the 380 and 475 μHz regions gives $\sqrt{3}/2$ with an accuracy better than 1%. This number was found in other GW Vir stars, as RXJ 2117+3412 and the central star of NGC 1501 (Bond et al. 1996), and is compatible with calculated trapping coefficients (Kawaler & Bradley 1994).

5. The damped oscillator hypothesis

When we discovered that the DFT was unstable, we also tried to explain such apparent time dependence of the

³ Note that these methods, which are in general much more reliable than the DFT of the period spectrum, can completely fail when they are applied to a period list erroneous and/or incomplete, as it can be in our case. For this reason the hypothesis that the signals are equally spaced in period (and not in frequency) can not be completely ruled out.

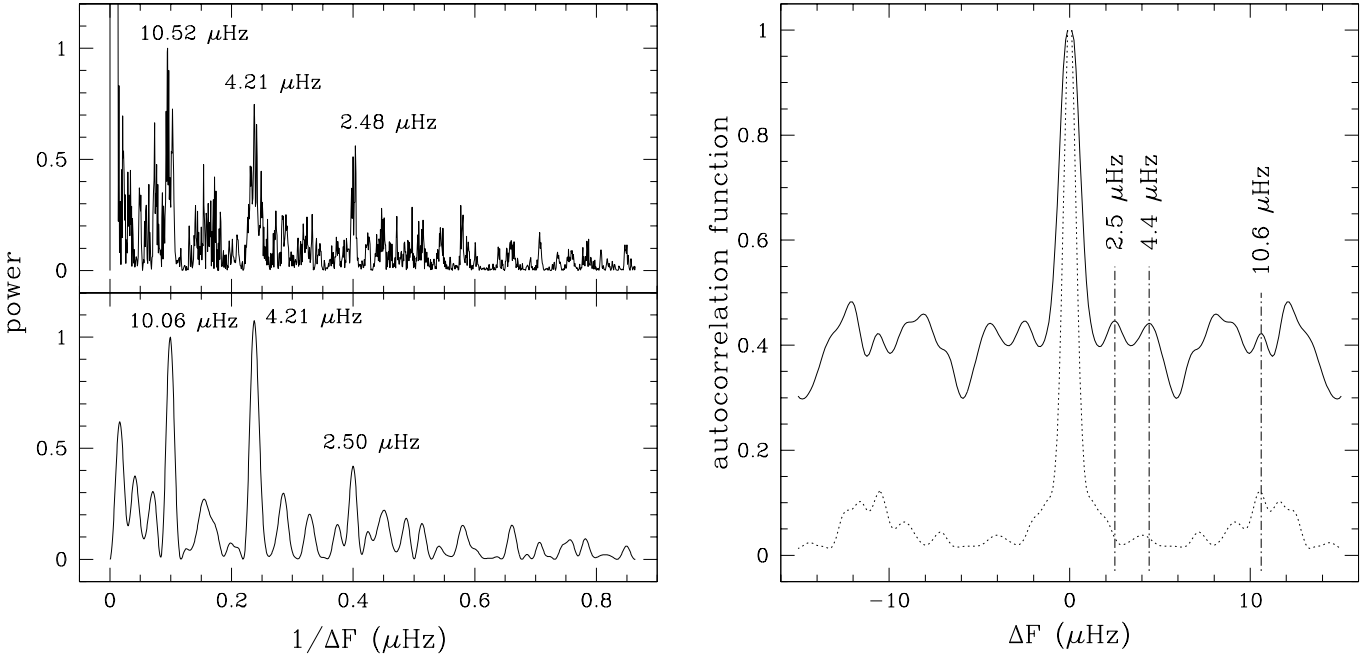


Fig. 6. Search for the frequency spacing.

Left panels: power spectrum of the data amplitude spectrum using two different subsets of the DFT: $350 \leq f \leq 1000 \mu\text{Hz}$ (all the signals, top panel) or $440 \leq f \leq 500 \mu\text{Hz}$ (only high-power signals, bottom panel). The power is normalized to the peak at 10.52 (10.06) μHz , which is partially due to the one day aliases (see the text). Right panel: autocorrelation function of the data DFT using the same subset as in the left bottom panel. The peaks between about 8 and $13 \mu\text{Hz}$ are partially due to the spectral window, as it is highlighted by the autocorrelation of the spectral window (dotted line).

DFT with a completely different quasi-periodic approach. We considered the hypothesis that the DFT temporal instability was real and due to a very short life time of the oscillations, which were continuously excited and damped.

We therefore applied to the HS 2324 data the Linear State Space model developed by Michael König for the analysis of X-ray variability of AGN (König & Timmer 1997, König et al. 1997). The current version of this program requires uninterrupted and equally spaced datasets. Moreover, in order to provide reliable results, the time scales to be investigated must be sampled at least ten times. The only part of our light curve which fulfills these criteria (JD 94–94.9, after rebinning with 200s) can be actually fitted with a period of 2134s and a damping time of approximately 3.5 periods. A further attempt has been done using a larger nearly uninterrupted part of the light curve (JD 94–95.7), filling the small gaps with white noise or with synthetic data (both techniques give same results). The results are slightly different in this case: 2154s and 3.1 periods. In both cases from a K-S test the residual is white noise with over 90% probability. If we try to find a secondary period the results are unreliable (damping time longer than the dataset), but in any case the inclusion of more frequencies does not improve the fit.

In Figure 8 the fit from the Linear State Space model is compared with the multisinusoidal fit: the quality is

comparably good. Despite this partial success, we cannot demonstrate that the damping time found is really a fundamental quantity, constant over at least some days. We would need several datasets (ideally, but not necessarily coherent) of at least one day length to reject or corroborate this hypothesis. Moreover, the excitation time-scale obtained from the Linear State Space model appears to be very short respect to the growth rates obtained from GW Vir non-adiabatic models. For these reasons the present results are not convincing enough to abandon the DFT results. On the other hand, the inviting advantage of the quasi-periodic approach is the small number of parameters required to describe the light curve. Unstable power spectra have been found also in other luminous PG 1159 stars (e.g. RXJ2117+3412) and [WC] CSPN (e.g. NGC 1501) variables. Changes were observed down to the time resolution of several days (Bond et al. 1996, Table 6).

6. Summary and discussion

The results of our multisite campaign clearly show that the power spectrum of HS 2324 contains several periodic signals (about 20 or more). We therefore may exclude binarity to explain its variability, as already suggested by Handler et al. (1997). The frequencies and amplitudes are comparable with those of the GW Vir stars. If we con-

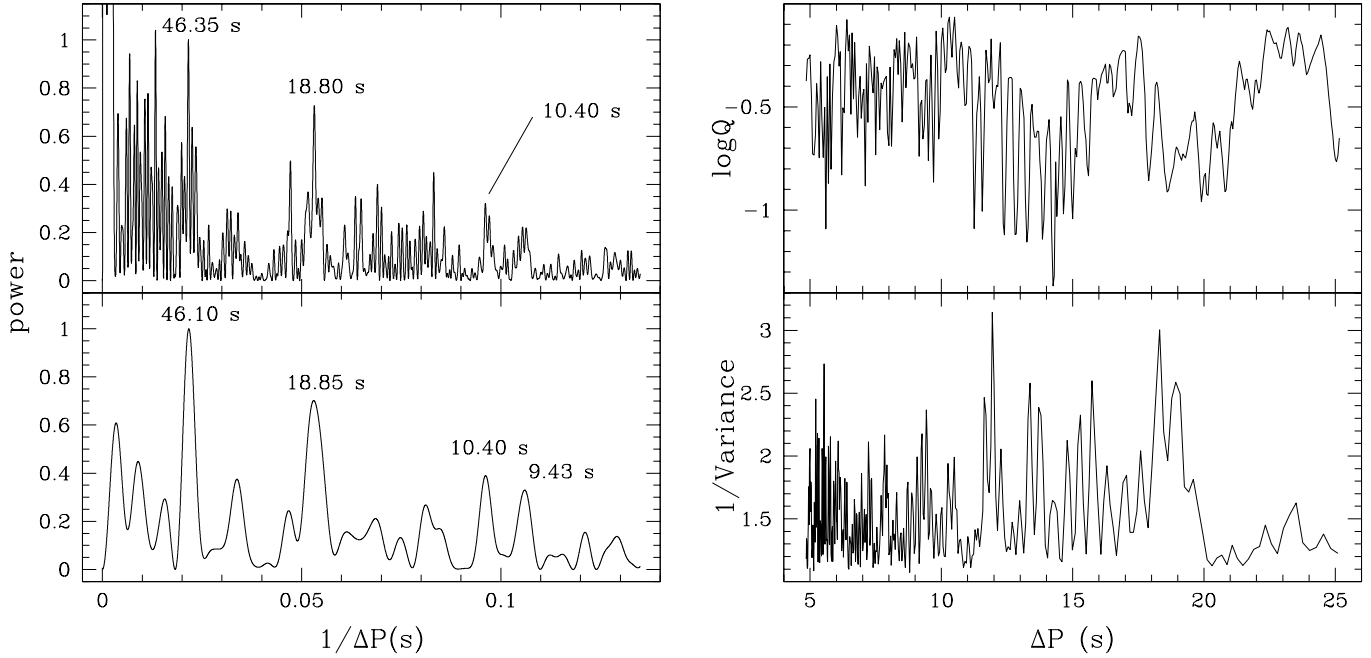


Fig. 7. Search for the period spacing.

Left panels: Fourier transform of the period spectrum (amplitude spectrum in the period domain) in the period range $1000 \leq P \leq 2857$ s (top) and $2000 \leq P \leq 2273$ s (bottom). The power is normalized to the peak at 46.3 (46.1) s, which is mainly due to the one day aliases in the main power region between 2000 and 2273 s. The peaks at 18.8 and 10.4 s might be due to the $l=1$ and $l=2$ period spacing. The peak at 9.4 s is the first harmonic of the 18.8 s signal. Right panels: Kolmogorov-Smirnov test (top) and Inverse Variance test (bottom) applied to the first 12 frequencies listed in Table 2 (excluding the linear combination region). Both tests do not show any significant value for the period spacing.

sider also that HS 2324 is spectroscopically classified as a PG 1159 star, the immediate interpretation is that its variability is due to high overtone g-mode pulsations.

The high H abundance detected in HS 2324, about 17% in mass (Dreizler 1998), is a very interesting and unique (up to now) element, which might help to shed light upon the driving mechanisms of the GW Vir stars. As discussed in the introduction, the presence of H was generally considered as an inhibitor of pulsations (Stanghellini et al. 1991). But this result was rather speculative because, until a few years ago, no H-rich PG 1159 stars were known. With HS 2324 this question has gained importance. Presently the real effects of the presence of H appear to be less severe from preliminary models of H-rich GW Vir stars (Saio 1996, Gautschy 1997). On the other hand, the detection of hydrogen in the atmosphere of HS 2324 does not necessarily imply that hydrogen is present also in the driving regions. However, HS 2324 belongs to the subclass of luminous PG 1159 stars which still show mass loss effects in strong UV/FUV lines (Koesterke & Werner 1998, Koesterke et al. 1998). It is highly probable that HS 2324 is also affected by mass loss which would inhibit an abundance gradient due to gravitational settling. It is therefore plausible that the atmospheric composition is also representative for the driving region. An unambiguous detection of mass loss and the determination of the mass loss

rate has to await FUSE (Far Ultraviolet Spectroscopic Explorer) observations of the O VI resonance lines.

However, the asteroseismological analysis is hampered by the fact that the DFT appears to be unstable in time. In principle this is not a new phenomenon: it has been observed in the light curve of all luminous PG 1159 and [WC] variables (the term "variable variables" was therefore coined by S. D. Kawaler). But in our case, as discussed in Section 3.1, this fact is probably due to a poor frequency resolution caused by an insufficient coverage.

If this interpretation is correct, it is not possible to obtain definite precision asteroseismology results from our data set. Nevertheless a spacing of the signals is probably present in the DFT and can be explained in two different ways. The most likely hypothesis is that we see the frequency spacing produced by the stellar rotation with a period $P_{ROT} = 2.31 \pm 0.15$ days. The second possibility, which can not be completely excluded, is that we see the period spacing between successive overtones. In this case the period spacings, equal to 18.8 ($l=1$) and 10.4 ($l=2$) s, would imply a stellar mass of 0.67 ($l=1$) and 0.70 M_{\odot} ($l=2$) using the interpolation formula of Winget et al. (1991). This asteroseismological mass would be higher than the 0.59 M_{\odot} value, found from spectroscopy plus evolutionary tracks (Dreizler et al. 1996). But this discrepancy would not be very significant as it is possible that

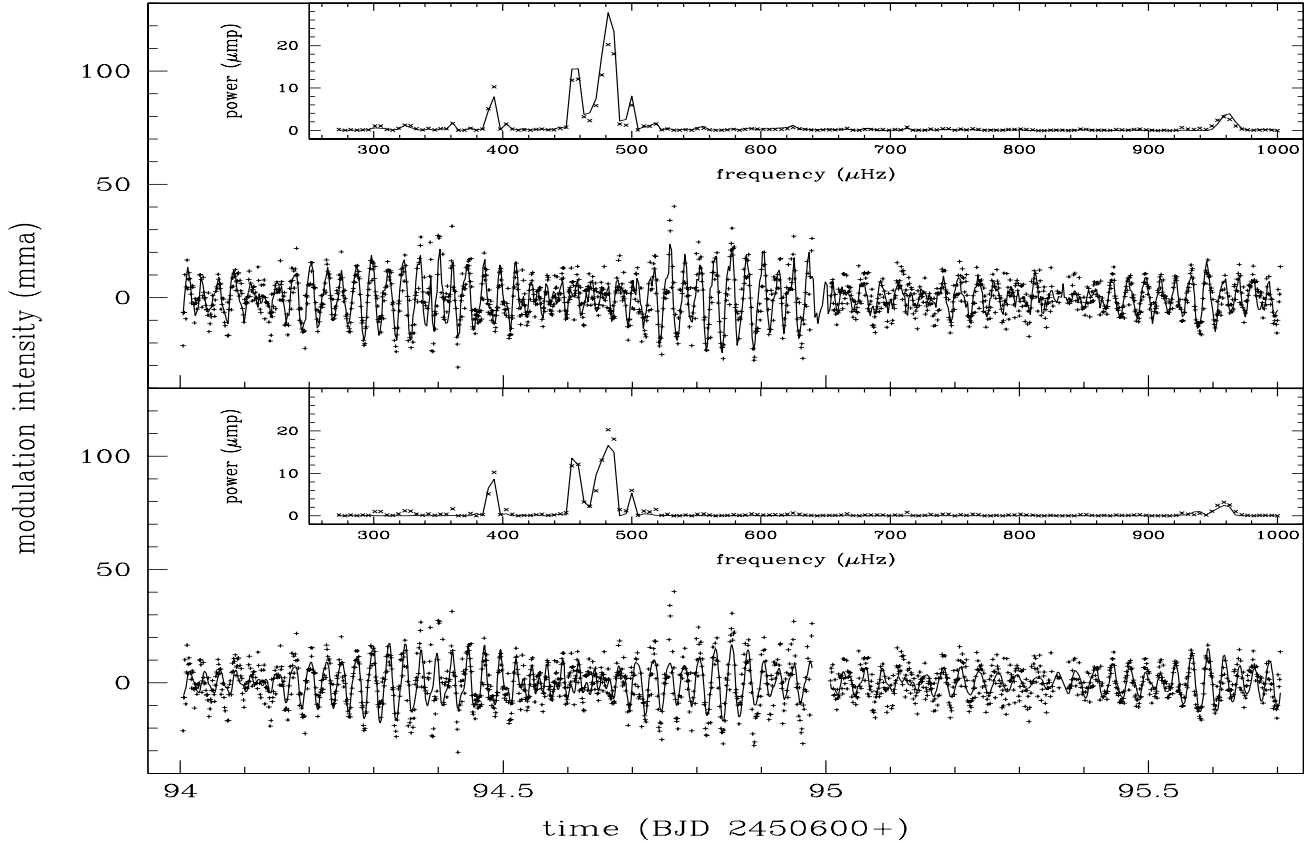


Fig. 8. Damped oscillator (up) vs 19 sinusoids function (down) in the best part of the light curve (BJD 94.0–95.7). Both the synthetic light curves (main panels) and DFTs (window panels) are shown and compared with the HS 2324 data (crosses).

the interpolation formula of Winget et al. (1991) needs some adjustment because of the peculiar composition of HS 2324.

In an alternative interpretation we assumed that the DFT instability was real and we applied the Linear State Space model (König & Timmer 1997) to investigate the quasi-periodic nature of these variations. As discussed in Section 5, this approach is also partially successful, but it also requires new longer observations to be confirmed. At the moment we can only speculate about the physical interpretation. Do we see the coupling time between different g-modes or the damping of a single mode? In principle, the quasi-periodic nature of HS 2324 could even endanger the interpretation as g-mode pulsations.

In conclusion both possible interpretations of the apparent DFT instability need a new bigger observational effort, which could be realized only with a larger number of telescopes in a WET-like campaign. If we adopt the hypothesis that the DFT instability is only apparent, it is also possible to estimate the duration needed for such a campaign in order to be able to separate all the frequencies. If all the $l=1$ and $l=2$ frequencies were excited in the region between 450 and 500 μHz , where most power

is concentrated, the average frequency separation would be about 0.4 μHz . In a more realistic case, if only 50% of the frequencies were excited (as in PG 1159, which is the GW Vir star with the largest number of detected modes), a frequency resolution of about 0.8 μHz would be enough. Therefore we would require a data set with a time base of about 1.7 times the data set analyzed in this paper.

Acknowledgements. This research was partially supported by the Italian “Ministero per l’Università e la Ricerca Scientifica e Tecnologica” (MURST) and by the EU grant ERBFMMACT980343; by the Deutsche Forschungs Gemeinschaft under travel grant DR 281/8-1; by the Austrian Fonds zur Förderung der wissenschaftlichen Forschung under grant S7304-AST; and by the Chinese National Science Foundation. S.D. would like to thank Ralf Geckeler (University of Tübingen) for providing his excellent CCD-photometry analysis program package as well as Katja Potschmidt (University of Tübingen) for her introduction to the time series analysis package of M. König and for her fruitful discussions. R.S. would like to thank Steven Kawaler (Iowa State University, Ames), Thomas Strauss (Astronomical Observatory of Capodimonte, Naples), Pawel Moskalik (Copernicus Astronomy Center, Warsaw) and Scot Kleinman (University of Texas at Austin) for interesting discussions, and Adalberto Piccioni (University of

Bologna) for the availability of the Loiano photometer. R.S. and S.D. are grateful to the Vienna Delta Scuti Network Group for their kind hospitality during the short stay in April–May 1998, in which part of this work has been done. The same applies to G.H.’s stay at the University of Tübingen in December 1997.

References

- Bond H.E., Kawaler S.D., Ciardullo R., et al., 1996, *AJ* 112, 2699
- Bradley P.A., 1998, *Baltic Astronomy* vol.7, 355
- Bradley P.A., Dziembowski W.A., 1996, *ApJ* 462, 376
- Ciardullo R., Bond H.E., 1996, *AJ* 111, 2332
- Deeming T.J., 1975, *Ap&SS* 36, 137
- Dreizler S., 1998, *Baltic Astronomy* vol.7, 77
- Dreizler S., Werner K., Heber U., Engels D., 1996, *A&A* 309, 820
- Dreizler S., Heber U., 1998, *A&A* 334, 618
- Gautschy A., 1997, *A&A*, 320, 811
- Handler G., Kanaan A., Montgomery M.H., 1997, *A&A* 326, 692
- Kawaler S.D., 1988, in *Advances in Helio and Asteroseismology*, Proc. IAU Symp. 123, eds. J.J. Christensen-Dalsgaard and S. Frandsen (Reidel:Dordrecht), 329
- Kawaler S.D., Bradley P.A., 1994, *ApJ* 427, 415
- Koesterke L., Dreizler S., Rauch T., 1998, *A&A* 330, 1041
- Koesterke L., Werner K., 1998, *ApJ* 500, L55
- König M., Timmer J., 1997, *A&AS* 124, 589
- König M., Staubert R., Wilms J., 1997, *A&A* 326, L25
- Kurtz D.W., 1985, *MNRAS* 213, 773
- Loumos G.L., Deeming T.J., 1978, *Ap&SS* 56, 285
- Moskalik, P., 1993, *Baltic Astronomy* vol.2, 485
- Nather R.E., Winget D.E., Clemens J.C., Hansen C.J., Hine B.P., 1990, *ApJ* 361, 309
- Napiwotzki R., Schönberner D., 1991, *A&A* 249, L16
- O’Donoghue D., 1994, *MNRAS* 270, 222
- Pesnell W.D., 1985, *ApJ* 292, 238
- Press W.H., Teukolsky S.A., Vetterling W.T., Flannery B.P., 1992, *Numerical Recipes*, (Cambridge Univ. Press: Cambridge)
- Saio H., 1996, in *Hydrogen-Deficient Stars*, eds. U.Heber and C.S.Jeffery, *ASP Conf. Series* 96, 361
- Silvotti R., 1996, *A&A* 309, L23
- Stanghellini L., Cox A.N., Starrfield S., 1991, *ApJ* 383, 766
- Starrfield S., Cox A.N., Kidman R.B., Pesnell W.D., 1984, *ApJ* 281, 800
- Stumpff P., 1980, *A&AS* 41, 1
- Werner K., 1992, in *Atmospheres of Early-type Stars*, eds. U. Heber and C.S. Jeffery, *Lecture Notes in Physics* 401, (Springer-Verlag: Heidelberg), 273
- Werner K., Bagnick K., Rauch T., Napiwotzki R., 1997, *A&A* 327, 721
- Winget D.E., Nather R.E., Clemens J.C., et al., 1991, *ApJ* 378, 326
- Winget D.E., Nather R.E., Clemens J.C., et al., 1994, *ApJ* 430, 839